Tellus (1997), 49B, 393–408
Printed in UK – all rights reserved

TELLUS
ISSN 0280–6509

Contribution of China to the global carbon cycle since the last glacial maximum

Reconstruction from palaeovegetation maps and an empirical biosphere model

By CHANGHUI PENG[1,2] and MICHAEL J. APPS[2]*, [1]*Laboratoire de Botanique Historique & Palynologie, UA CNRS 1152, Faculté de St Jérôme, 13397 Marseille Cedex 20, France,* [2]*Natural Resources Canada, Canadian Forest Service, 5320–122 Street, Edmonton, Alberta T6H 3S5 Canada*

(Manuscript received 28 October 1996; in final form 18 March 1997)

ABSTRACT

A better understanding of the long-term global carbon cycle requires improved estimates of the changes in terrestrial carbon storage (vegetation and soil) during the last glacial-interglacial transition. A set of reconstructions of palaeovegetation and palaeoclimate in China for the last glacial maximum (LGM) and the mid-Holocene (MH) allows us to use the Osnabrück biosphere model (OBM), which needs as input only 3 climatic parameters that are easily derivable from palaeodata, to reconstruct the past terrestrial carbon storage since the LGM. The change from the conditions of the LGM (colder and drier than present) to the MH (warmer and wetter than present) resulted in a gain of 116 Pg of terrestrial carbon in China mainly due to the build-up of temperate forest and tropical monsoon rain forest, and to the effects of changes in climate and CO_2 levels. However, a loss of 26 Pg of terrestrial carbon (which does not include anthropogenic disturbances) occurred in China between the MH and the present due to shifts in the area covered by the main vegetation types. Results also show that glacial-interglacial changes in climate and vegetation distribution, both associated with variations in the Asian monsoon system, significantly affected terrestrial carbon storage in China which strongly contributed to the global carbon cycle.

1. Introduction

The transition from the last glacial maximum (LGM) (about 21 000–18 000 years BP) to present interglacial conditions brought with it many changes in the global biogeochemical cycle. The CO_2 measurements from the Vostok Ice Core (Barnola et al., 1987) clearly indicate that the atmospheric CO_2 concentration has varied greatly over the last climatic cycle: cold glacial periods being associated with low CO_2 concentrations (about 200 ppm) and warm interglacial periods being associated with high CO_2 concentrations (about 270 ppm), which are near to that of pre-industrial time (about 280 ppm). The terrestrial biosphere plays an important rôle in the global carbon cycle (Smith et al., 1993; Sampson et al., 1993) as a modulator of changes in atmospheric CO_2. Concerns about the impacts of increasing the atmosphere's CO_2 concentration and future global warming on the terrestrial biosphere, as well as the interactions and feedbacks between the climate system and the terrestrial biosphere, have focused attention on our need to better understand past changes in terrestrial vegetation and carbon storage (Adams et al., 1990; Prentice and Fung, 1990; Sundquist, 1993).

The last glacial maximum (LGM) and the mid-Holocene (MH) are two key time slices for the

* Corresponding author.
E-mail: mapps@nofc.forestry.ca

reconstruction of past environments with known climate forcing. The LGM was characterized by extensive ice sheets in northern mid-latitudes, sea-surface temperatures generally colder than those at present, lower atmospheric CO_2 (about 200 ppm), and a sea level 120 m lower than that at present (Bartlein, 1988). Although the LGM represents a cold, low CO_2 world, it does not represent a mirror image of the future warm, high CO_2 one. The MH has been proposed as an analogue to possible future warm climates potentially induced by doubling the concentration of atmospheric CO_2 (Borzenkova and Zubakov, 1984; Kellogg, 1990; Butzer, 1980; Folland et al., 1990), but the analogue is false (IPCC, 1995). Because the Earth's orbital configuration was different from present, even if deglaciation was essentially completed by this time, ice-sheet extent and sea level were similar to the present, and the atmospheric CO_2 concentration according to ice-core records had stabilized within its pre-industrial range of 270–280 ppm (Barnola et al., 1987). At the MH summer insolation was higher than at present in the Northern Hemisphere, and total annual insolation was greater than at present at high latitudes (IPCC, 1995).

China, located between latitude 20 and 54°N and between longitude 75 and 130°E, has climate regimes ranging from perennial snow on the high western mountains to deserts in the western lowlands, and from cold temperate regions in the northeast to warm and humid tropics along the southern coast (Editors of the Teachers College of Northwest China, 1984). The climate of east-central China is characterized by alternations of East Asian summer and winter monsoons which are driven by the differential heating between the Asian continent and the Pacific Ocean to the east and southeast, and the Indian Ocean to the southwest (Gao et al., 1962). The monsoons support a unique set of ecosystems ranging from the boreal coniferous forest in the northeast to the tropical monsoon rain forest in the south. The climatic variability, topographic complexity, and natural ecosystem diversity give China an important rôle in global change studies (Ye et al., 1995).

Great efforts have been made to reconstruct the changes in paleoclimatic patterns and paleovegetation distributions (An et al., 1991; Shi et al., 1993; Wang and Sun, 1994; Winkler and Wang, 1994). However, the regional-scale reconstruction of glacial-interglacial terrestrial carbon of China has not been reported until now. A few global syntheses contain estimates of terrestrial carbon storage of China for the LGM (Adams et al., 1990; Prentice and Fung, 1990; Prentice et al., 1993; Van Campo et al., 1993; Esser and Lautenschlager, 1994; Peng et al., 1995a) and for the MH (Foley, 1995), but these estimates are based on inaccurate global data (Adams et al., 1990; Van Campo et al., 1993; Peng et al., 1995a) or coarse resolution general climate circulation models (GCMs) (Prentice and Fung, 1990; Prentice et al., 1993; Esser and Lautenschlager, 1994; Foley, 1995). The uncertainties in these reports arise not only from the uncertainties in the climate simulation themselves for the present or past, but also from their inability to take into account the dynamic processes of the carbon cycle (e.g., possible low-fertilization effect of low atmospheric CO_2 concentration on the net primary productivity). For these reason, the combined use of regional data and a biosphere carbon model was undertaken to reconstruct the terrestrial carbon dynamics during the glacial-interglacial transition.

A previous study (Peng et al., 1995a) demonstrated the ability of the Osnabrück biosphere model (OBM) to provide reconstruction of past terrestrial carbon storage from the global palaeodata of Frenzel et al., (1992) despite its limited and inadequate data for China. The objective of the present study is to use the OBM (Esser, 1987, 1991) modified by Peng et al. (1995a) and the Chinese palaeovegetation maps of An et al., (1991) and Shi et al., (1993), which are the best regional maps for China, to investigate the effects of past climatic change on vegetation distribution and long-term terrestrial carbon dynamics. We focus on the reconstruction of terrestrial carbon storage of China for the LGM, MH and present. The results are compared to those obtained from the carbon densities of Olson et al., (1985) and Zinke et al., (1986) for the present, as well as to other regional estimates of past terrestrial carbon storage during the same periods (Branchu et al., 1993; Monserud et al., 1995).

2. Model and data

2.1. Description of the Osnabrück biosphere model

The OBM developed by Esser (1987, 1991) and modified by Peng et al. (1995a) has a grid resolution of 0.5° × 0.5° (longitude × latitude) and is a dynamic, global-scale model of the carbon cycle. The model describes the major fluxes and pools of carbon in the terrestrial biosphere, depending on mean annual temperature, total annual precipitation and the atmospheric CO_2 concentration. A detailed description of the model and a discussion of its applicability to present conditions can be found in the original papers. A further application of this model to palaeodata is given in Peng et al., (1995a, b). Here, we report mainly on several important features and modifications made in this study.

The OBM identifies three pools of terrestrial carbon: herbaceous and woody live biomass, litter from herbaceous and woody material, and soil organic carbon. The carbon fluxes are net primary production (NPP), allocation of assimilates to the compartments of live biomass, litter production, litter decomposition, soil organic carbon production, and soil organic carbon decomposition. The structure of the OBM is depicted in Fig. 1.

The NPP calculated by the OBM is an equilibrium prediction representing the net carbon input from the atmosphere into the biosphere. The model assumes that vegetation change is in equilibrium with climate. The productivity of the potential vegetation is limited either by temperature or precipitation and can be estimated by the MIAMI model (Lieth, 1975) and modified by soil fertility (F_{soil}) and by a CO_2 fertilization factor (F_{CO_2}) (Esser, 1991). This latter factor, which summarizes the influence of the entire complex of ecological effects of the atmospheric CO_2 concentration, is important for understanding the glacial-interglacial biosphere carbon budget. It depends on the atmospheric CO_2 concentration (CO_2) and soil fertility (F_{soil}).

$$F_{soil} = \sum_{k=1}^{k(m)} f_k \times AS(m, k) / \sum_{k=1}^{k(m)} AS(m, k), \quad (1)$$

$$F_{CO_2} = A \times [(1 - e)^{(-R(CO_2 - 80))}], \quad (2)$$

$$A = (1 + F_{soil})/4,$$

$$R = -\ln((A - 1)/A) \times (1/240).$$

Here f_k is soil factor for soil unit k, and $AS(m, k)$ is the area (km^2) occupied by a soil unit k in a grid element m.

The CO_2 fertilization effect as described by the eq. (2) has proved to be reliable if used from pre-industrial to modern CO_2 concentration, but the extrapolation of this equation to lower glacial

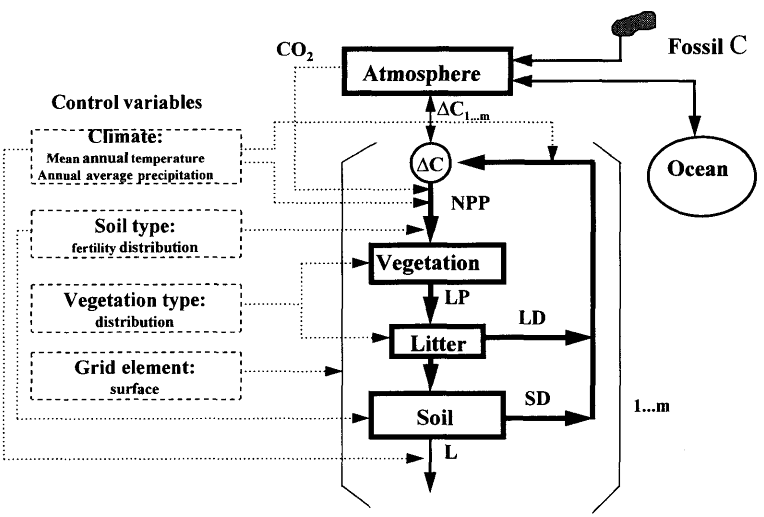

Fig. 1. Flow diagram of the Osnabrück Biosphere Model (OBM) (Esser, 1984, 1991) for calculation of carbon dynamics in the terrestrial biosphere. The control variables for calculation of carbon pools and fluxes are indicated by dotted arrows. The large brackets enclose the model structure on the level of each of the 0.5 grid elements that yields the carbon balance of each grid element (m) for one year ($C_{i,m}$). C: carbon; NPP: net primary productivity; LP: production of herbaceous and woody litter; LD: decomposition of litter; SD: decomposition of humic compounds in the soil; L: leaching of organic compounds; ΔC: net carbon exchange between the atmosphere and biosphere.

CO_2 concentration must be considered speculative (Esser, 1987, 1991). A further discussion of the CO_2 fertilization effect can be found in Esser and Lautenschlager (1994) and Peng et al. (1995a).

In the OBM, the vegetation biomass is calculated by an empirical relationship between NPP and mean stand age of vegetation. Mean stand age represents the approximate average turnover time of the vegetation, and is derived from DATAVW which is a comprehensive literature database of net primary productivity, biomass and decomposition rates developed at the University of Osnabrück, Germany. A few gaps are filled using a ranking method (Esser, 1984). Litter production and decomposition, and soil organic carbon production and decomposition are functions of mean annual temperature, total annual precipitation, atmospheric CO_2 concentration, soil fertility, and vegetation type.

We do not take into account the effect of land-use changes when estimating the potential carbon storage in vegetation, litter and soil pools. The losses of dissolved and particulate organic carbon through leaching or deposition are generally negligible (Schlesinger and Melack, 1981; Schlesinger, 1985).

2.2. Data

The data sets required by the model are atmospheric CO_2 concentration, mean annual temperature, total annual precipitation, potential vegetation types and soil types at each grid cell. These data sets came from the various sources described below.

2.2.1. Atmospheric CO_2 concentration. The CO_2 concentration of the atmosphere was set to 280 ppm (pre-industrial value) for the present time, 270 ppm for the mid-Holocene (MH), and 200 ppm for last glacial maximum (LGM), based on the CO_2 measurements from the Vostok Ice Core (Barnola et al., 1987). Sea level was assumed to be 120 meters below present at the LGM (Moore et al., 1981; An et al., 1991; Winkler and Wang, 1994; Peltier, 1994), leading to an increase of $1.15 \cdot 10^{12}$ m^2 in the continental area for China. Assuming the atmosphere acts as an unlimited carbon source for terrestrial pools, we obtained the initial values for each pool using a fixed atmosphere CO_2 concentration of 280 ppm for the present, 270 ppm for the MH, and 200 ppm for the LGM. The pre-run procedure requires considerable computing (about 1500 simulated years) in order to obtain stable soil pools and prevent subsequent model drift in the continued model run.

2.2.2. Vegetation data. Modern vegetation map. The map of modern vegetation distributions in China (Wu et al., 1980) provides the most complete reference for the distribution of nine potential vegetation types (Fig. 2a, Table 2) which were digitized at the $0.5° \times 0.5°$ grid level. Because the map is based on potential vegetation, land-use is not included in this map. The vegetation types displayed include (1) boreal coniferous forest (BOCF), (2) coniferous and deciduous broad-leaved mixed forest (CDMF), (3) deciduous and broad-leaved forest (DBLF), (4) deciduous and evergreen broad-leaved mixed forest (DEMF), (5) desert and semidesert (DESE), (6) highland vegetation (HLVE), (7) subtropical evergreen broad-leaved forest (SEBF), (8) steppe and highland steppe (STEP), and (9) tropical monsoon rain forest (TMRF). The mean stand age (years) of each vegetation type and the share factors needed to calculate herbaceous and woody portions of production were derived from Esser (1991, Table 31.6).

Palaeovegetation maps. For past vegetation we rely primarily on the published palaeovegetation maps of Shi et al. (1993) for the MH (Fig. 2b) and An et al. (1991) for the LGM (Fig. 2c). We deem these two maps to be the best such regional maps for China. They were compiled from various regionally-specific data sources including radiocarbon-dated pollen data, paleosols, archaeological data, palaeolimnology, sea-level change and ice cores (see Fig. 1 in Shi et al., 1993). Although the data, methods and stratigraphy on which the reconstructions are based are not clearly described and their reliability not indicated by An et al. (1991), the LGM period, with dominant steppes and desert, and a disappearance of monsoon rain forest together with a major shift of vegetation regions towards the southeast as compared with their modern patterns, is consistent with independent palynological records (Zheng, 1986; Xu et al., 1987; Liu, 1988; Wang and Sun, 1994), and certainly represents a more reliable

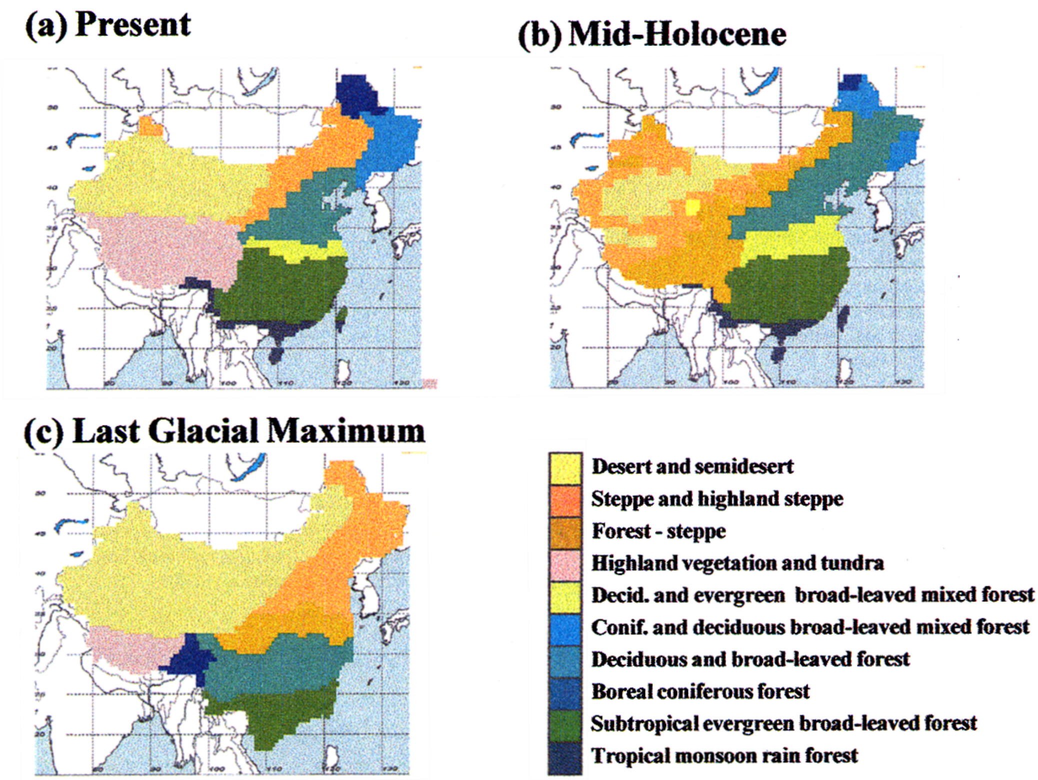

Fig. 2. (a) Modern potential vegetation distribution in China (Wu et al., 1980); (b) reconstruction of paleovegetation of China at the mid-Holocene (MH) (Shi et al., 1993); and (c) reconstruction of paleovegetation of China at the Last Glacial Maximum (LGM) (An et al., 1991).

regional reconstruction than the global palaeovegetation maps of Adams et al. (1990) and Frenzel et al. (1992).

The palaeovegetation map of Shi et al. (1993) for the MH contains nine vegetation types (Table 4). Comparing this map to the modern vegetation distribution (Table 2), we find that highland vegetation (HLVE) has disappeared and forest-steppe (FOST) has been added. The palaeovegetation map of An et al. (1991) provides the distribution of seven main vegetation types for the last glacial maximum (LGM) (Table 5). The tropical monsoon rain forest (TMRF), and deciduous and evergreen broad-leaved mixed forest (DEMF) disappeared completely from China at this time. Both the above palaeovegetation maps were digitized at the $0.5° \times 0.5°$ grid using the same method reported by Peng et al. (1995a). The mean stand age (years) of each vegetation type and the biomass share factor are reported in Table 1 assuming that these values are the same as present for corresponding vegetation types.

2.2.3. Climate data. Modern climatic data, including mean annual temperature (T_{present}) and total annual precipitation (P_{present}) were obtained from the revised version of the IIASA database (Leemans and Cramer, 1991) at a $0.5° \times 0.5°$ grid scale.

For the MH, mean annual temperature and total annual precipitation anomalies (ΔT_{MH} and ΔP_{MH}) were deduced directly from palaeovegetation in China by Shi et al. (1993) in order to ensure a good correspondence between the vegetation and climate. The average value of these climatic parameters was calculated for each modern vegetation type and attributed to a corresponding palaeovegetation type, in order to

Table 1. *The major vegetation types used in this study*

Code	Vegetation type	Mean stand age	H_h	Veg-c density low	Veg-c density medium	Veg-c density high	Soil-c density low	Soil-c density medium	Soil-c density high
BOCF	boreal coniferous forest	100	0.34	4.4	8.7	11.7	12.7	16.6	20.5
CDMF	coniferous and deciduous broad-leaved mixed forest	130	0.29	6.0	10.0	14.0	10.5	13.0	15.5
DBLF	deciduous and broad-leaved forest	150	0.44	8.0	10.0	14.0	12.7	15.2	17.7
DEMF	deciduous and evergreen broad-leaved mixed forest	150	0.38	8.0	10.0	14.0	12.7	15.2	17.7
DESE	desert and semidesert	5	0.85	0.2	0.45	0.85	3.3	4.6	5.9
FOST	forest-steppe	25	0.53	2.0	4.1	7.3	6.7	7.3	7.9
HLVE	highland vegetation	10	0.70	0.5	0.8	1.3	7.3	9.2	10.9
SEBF	subtropical evergreen broad-leaved forest	200	0.37	6.0	10.0	14.0	12.3	13.3	14.2
STEP	steppe and highland steppe	1	1.0	0.5	1.0	2.4	11.6	12.3	13.0
TMRF	tropical monsoon rain forest	200	0.37	10.0	14.0	17.0	9.5	10.4	11.3

Mean stand age (years) of vegetation and the NPP share factor for herbaceous H_h were derived from Esser (1991, in Table 31.6). The NPP share factor for woody H_w is simply calculated from 1-H_h. The vegetation carbon densities (kg/m^2) are from Olson et al. (1985) and soil carbon densities (kg/m^2) are from Zinke et al. (1986).

calculate climatic anomalies. We have interpolated these anomalies to the $0.5° \times 0.5°$ grid point using weighted averaging with a large radius (5°). The mean annual temperature (T_{MH}) and total annual precipitation (P_{MH}) were then obtained by adding these anomalies to the modern data.

$$T_{MH} = T_{present} + \Delta T_{MH}, \tag{3}$$

$$P_{MH} = P_{present} + \Delta P_{MH}. \tag{4}$$

This stepwise procedure was developed to preserve the influence of topography in China. Generally, it is estimated that the T_{MH} was higher than present about by 1°C in south China, 2.5°C in east China and by 3–4°C in north China and northeast China, much higher than the average value for the northern hemisphere (1.5°C) during 6500–7000 years BP estimated by Frenzel et al. (1992). A warming of 4–5°C was recorded in the Tibet Plateau.

Similarly, the anomalies of the mean annual temperature(ΔT_{LGM}), and total annual precipitation (ΔP_{LGM}) for the last glacial maximum (LGM) were digitized at the $0.5° \times 0.5°$ grid based on the relationship between the palaeovegetation map and climatic parameters reconstructed by An et al. (1991). Mean annual temperature (T_{LGM}), and total annual precipitation (P_{LGM}) were obtained by adding the LGM anomalies to the revised version of the IIASA modern climate (Leemans and Cramer, 1991) database (called T_{preset}, $P_{present}$):

$$T_{LGM} = T_{present} + \Delta T_{LGM}, \tag{5}$$

$$P_{LGM} = P_{present} + \Delta P_{LGM}. \tag{6}$$

To avoid negative precipitation values in MH and LGM, in a few instances, we multiplied current annual precipitation values by adjusted precipitation anomalies (for more detail see Esser and Lautenschlager, 1994). Preliminary estimations showed that the T_{LGM} in north China might have been 10–12°C lower than it is now, and the P_{LGM} might be less than 50% its present value (An et al., 1991). However, we did not take into account the direct effects of low CO_2 on canopy conductance. As a consequence estimates of precipitation changes for the LGM may be slightly overestimated because of decreases in stomatal conductance and transpiration rates in response to increases in CO_2 concentration from the LGM to the present (Beerling and Woodward, 1993).

2.2.4. Soil data. The soil data (Zobler, 1986) were based on the soil map of the world (FAO-UNESO, 1974) which is given on a $1° \times 1°$ grid scale. The soil units of this map were interpolated to a $0.5° \times 0.5°$ grid scale as required by the OBM. The soil fertility factor (F_{soil}) was derived by comparing the measured net primary production of the soil with NPP calculated from climate only (Esser, 1991). The soil types that are not in Table 31.4 of Esser (1991) were assumed to have a soil fertility factor (F_{soil}) of 1 (McGuire et al., 1993). Because of the lack of soil information for the MH and LGM, we simply used the same soil map as for the present time and assumed that the soil fertility factor remained constant for today, the MH and LGM. This assumption may be inappropriate for the LGM because soil may have been less developed during that period. For areas which are inundated now but were exposed by sea level depression (−120 m) during the LGM, we derived values from the Zobler (1986) database using distance-weighted and averaged interpolation.

3. Results

3.1. Modern distribution of terrestrial carbon storage in China

Table 2 shows that total modern terrestrial carbon storage in China is estimated at 157.9 Pg (57.9 Pg in vegetation and 100.0 Pg in soil). The highest carbon storages occur respectively in subtropical evergreen broad-leaved forest (SEBF) with 59.0 Pg, and deciduous and broad-leaved forest (DBLF) with 20.0 Pg, due to their larger area and higher carbon density. The lowest carbon storages are found in the boreal coniferous forest (BOCF) with 3.1 Pg and deciduous and evergreen broad-leaved mixed forest (DEMF) with 7.1 Pg, due to their small areas. The desert and semidesert (DESE) occupies the largest area at 24% of the study area (about $9.68 \cdot 10^{12}$ m^2), but it contains only 9.2% of the total carbon storage in China.

3.2. Model testing

Using the estimates of vegetation carbon densities by Olson et al. (1985) and soil carbon densities by Zinke et al. (1986) (Table 1), and taking into account the area for corresponding ecosystems, we estimated (Table 3) that total terrestrial carbon storage ranges between 116.9 and 182.8 Pg (including 31–67 Pg in vegetation and 85–116 Pg in soils). Note that low and high values indicate the variability of carbon storage due to climatic and other biotic factors within a given ecosystem rather than statistical error. We compared our model-based estimates of total carbon storage in vegetation and soil (Table 2) to that of global data-based estimates (Table 3) under the current climate. It seems that the OBM overestimates the vegetation carbon storage in subtropical evergreen broad-leaved forest and soil carbon storage in coniferous and deciduous broad-leaved mixed forest. It appears to underestimate the soil carbon storage in boreal coniferous forest and steppe. The simula-

Table 2. *Reconstruction of present vegetation area and total carbon storage (Tot-C) including carbon in vegetation (Veg-C) and in soil (Soil-C) calculated using the OBM model (Esser, 1991) and modern vegetation map (Wu et al., 1980)*

Code	Vegetation type	Area (10^{12} m^2)	Tot-C (Pg C)	Veg-C (Pg C)	Soil-C (Pg C)
BOCF	boreal coniferous forest	0.24	3.1	0.8	2.4
CDMF	coniferous and deciduous broad-leaved mixed forest	0.57	14.1	3.9	10.2
DBLF	deciduous and broad-leaved forest	0.97	20.0	7.8	13.0
DEMF	deciduous and evergreen broad-leaved mixed forest	0.33	7.1	3.0	4.0
DESE	desert and semidesert	2.31	14.5	1.0	13.5
HLVE	highland vegetation	2.03	16.9	1.1	15.8
SEBF	subtropical evergreen broad-leaved forest	1.72	59.0	33.7	25.3
STEP	steppe and highland steppe	1.13	12.5	0.9	11.5
TMRF	tropical monsoon rain forest	0.38	10.6	6.4	4.2
	total	9.68	157.9	57.9	100.0

Table 3. *The carbon storage in vegetation (Veg-C, Pg C) and soil (Soil-C, Pg C) for 9 ecosystems (Wu et al., 1980) are estimated using the vegetation carbon densities of Olson et al. (1985) and soil carbon densities of Zinke et al. (1986) at 3 levels (low, medium and high in Table 1) for present-day China*

		Area	Veg-C			Soil-C		
Code	Vegetation type	(10^{12} m^2)	low	medium	high	low	medium	high
BOCF	boreal coniferous forest	0.24	1.1	2.1	2.8	3.1	4.0	4.9
CDMF	coniferous and deciduous broad-leaved mixed forest	0.57	3.4	5.7	8.0	6.0	7.4	8.8
DBLF	deciduous and broad-leaved forest	0.97	7.8	9.7	13.6	12.3	14.7	17.2
DEMF	deciduous and evergreen broad-leaved mixed forest	0.33	2.6	3.3	4.6	4.2	5.0	5.8
DESE	desert and semidesert	2.31	0.5	1.1	2.0	7.6	10.6	13.6
HLVE	highland vegetation	2.03	1.0	1.6	2.6	14.8	18.7	22.1
SEBF	subtropical evergreen broad-leaved forest	1.72	10.3	17.2	24.1	21.2	22.9	24.4
STEP	steppe and highland steppe	1.13	0.6	1.1	2.7	13.1	13.9	14.7
TMRF	tropical monsoon rain forest	0.38	3.8	5.3	6.5	3.6	3.9	4.3
	total carbon storage		31.1	47.1	66.9	85.9	101.1	115.8

tion of total potential terrestrial carbon storage by the OBM, however, is within the range of observational uncertainty. Hence we conclude that the OBM model adequately reproduces the expected value of modern potential terrestrial carbon storage in China.

3.3. *Change in terrestrial carbon storage from the MH to the present time*

As shown in Fig. 3 and Table 4, total terrestrial carbon storage in China for the MH was 183.4 Pg (70.6 Pg in vegetation and 112.8 Pg in soil), compared to 157.9 Pg (57.9 Pg in vegetation and 100.0 Pg in soil) at the present. The loss of 25.5 Pg of carbon storage between the MH and present is significant. (We note that this loss would be even greater for modern times if the potential vegetation were modified to account for land-use and other anthropogenic disturbances.) The main contributions to the loss estimated here are the decrease of 21.7 Pg in the deciduous and broad-leaved forest (DBLF), 31.0 Pg in the forest-steppe (FOST) and 8.2 Pg in the deciduous and evergreen broad-leaved mixed forest (DEMF). These are partly compensated by the extension of highland vegetation (HLVE), coniferous and deciduous broad-leaved mixed forest (CDMF) and desert (DESE), which together increase the carbon storage by 28.4 Pg at the present time. The boreal coniferous forest (BOCF) has expanded greatly in area since the MH, but its still small area results in a gain of only 2.6 Pg of carbon storage (Fig. 4).

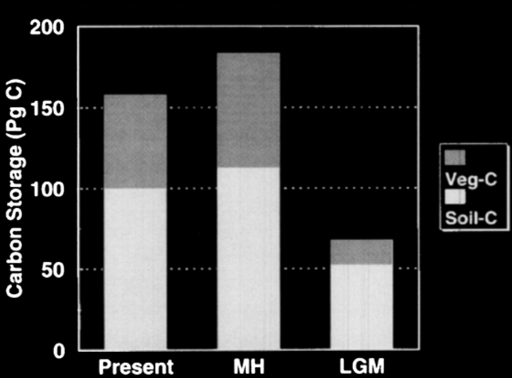

Fig. 3. Change in terrestrial carbon storage in China from the LGM to present.

3.4. *Change in terrestrial carbon storage from the LGM to the MH*

As shown in Fig. 3 and Table 5, total terrestrial carbon storage in China in the LGM was only 67.9 Pg (15.5 Pg in vegetation and 52.4 Pg in soil), compared to 183.4 Pg (70.6 Pg in vegetation and 112.8 Pg in soil) at the MH. This implies a gain of 115.6 Pg in carbon storage from LGM to MH. This is comparable to the estimated 154 Pg

Table 4. *Reconstruction of mid-Holocene (MH) vegetation area and total carbon storage (Tot-C) including carbon in vegetation (Veg-C) and in soil (Soil-C), calculated by using the OBM (Esser, 1991) and palaeodata from Shi et al. (1993)*

Code	Vegetation type	Area (10^{12} m^2)	Tot-C (Pg C)	Veg-C (Pg C)	Soil-C (Pg C)
BOCF	boreal coniferous forest	0.06	0.5	0.1	0.4
CDMF	coniferous and deciduous broad-leaved mixed forest	0.37	9.9	2.9	7.1
DBLF	deciduous and broad-leaved forest	1.59	41.7	15.2	26.5
DEMF	deciduous and evergreen broad-leaved mixed forest	0.68	15.2	6.4	8.8
DESE	desert and semidesert	1.20	7.6	0.5	7.1
FOST	Forest-steppe	2.01	31.0	3.6	27.4
SEBF	subtropical evergreen broad-leaved forest	1.67	57.7	34.7	23.1
STEP	steppe and highland steppe	1.75	9.5	0.6	8.9
TMRF	tropical monsoon rain forest	0.35	10.3	6.6	3.7
	total	9.68	183.4	70.6	112.8

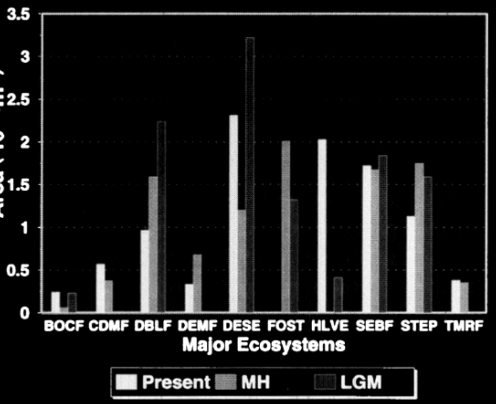

Fig. 4. Change in area of major ecosystem in China for the LGM, MH and present. The area unit is in 10^{12} m^2 and the symbols are defined in Table 1 (BOCF: boreal coniferous forest; CDMF: coniferous and deciduous broad-leaved mixed forest; DBLF: deciduous and broad-leaved forest; DEMF: deciduous and evergreen broad-leaved mixed forest; DESE: desert and semidesert; FOST: forest-steppe; HLVE: highland vegetation and tundra; SEBF: subtropical evergreen broad-leaved forest; STEP: steppe and highland steppe and TMRF: tropical monsoon rain forest).

increase in carbon for the whole of Africa from LGM to MH conditions reported by Branchu et al. (1993). The changes in terrestrial carbon storage from the LGM to the MH in China that we calculate are mainly due to (1) changes in vegetation areas, (2) the effects of change in climate and CO_2 levels, and (3) the influence of inundation at deglaciation. The build-up of modern tropical monsoon rain forest (TMRF) and deciduous and evergreen broad-leaved mixed forest (DEMF), which were completely absent during the LGM, resulted in an increase of 25.5 Pg total carbon storage. Additional contributions to MH carbon storage are made by 14 Pg increase in forest-steppe (FOST) and 38.7 Pg in subtropical evergreen broad-leaved forest (SEBF). The effects of changes in climate (warmer and wetter) and CO_2 fertilization (assumed with an increase of CO_2 concentration from 200 ppm at LGM to 270 ppm at MH) contributed an increase of 45.1 Pg C in the carbon storage of MH. However, the influence of inundation at deglaciation resulted in a decrease of 7.5 Pg C in vegetation and soil from the LGM to the MH.

3.5. Contribution of China to the global carbon cycle since the LGM

The size of the total terrestrial carbon pool estimated in China for the pre-industrial present (Fig. 5) comprises approximately 7% of the mean global carbon pool of 2167 ± 730 Pg C (i.e., 8.3% of the global vegetation pool of 700 Pg C and 6.8% of the global soil pool of 1467 Pg C) reported by Woodwell et al. (1995) based on various empirical estimations. At the MH, the size of the total terrestrial carbon pool estimated for China repres-

Table 5. *Reconstruction of last glacial maximum (LGM) vegetation area and total carbon storage (Tot-C) including carbon in vegetation (Veg-C) and in soil (Soil-C), calculated using the OBM (Esser, 1991) and palaeodata from An et al. (1991)*

Code	Vegetation type	Area (10^{12} m^2)	Tot-C (Pg C)	Veg-C (Pg C)	Soil-C (Pg C)
BOCF	boreal coniferous forest	0.23	2.1	0.5	1.7
DBLF	deciduous and broad-leaved forest	2.24	19.5	3.9	15.6
DEMF	deciduous and evergreen broad-leaved mixed forest	0.00	0.00	0.00	0.00
DESE	desert and semidesert	3.22	6.7	1.3	5.4
FOST	forest-steppe	1.30	17.0	4.8	12.2
HLVE	highland vegetation and tundra	0.41	0.03	0.01	0.02
SEBF	subtropical evergreen broad-leaved forest	1.84	19.0	4.8	14.2
STEP	steppe and highland steppe	1.59	3.5	0.2	3.3
TMRF	tropical monsoon rain forest	0.00	0.00	0.00	0.00
	total	10.83	67.9	15.5	52.4

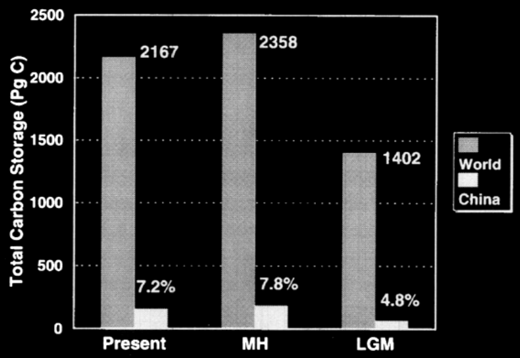

Fig. 5. The contribution of Chinese ecosystem to the global carbon budget for the LGM, MH and present. The percentage represents relative contribution of China to global terrestrial carbon storage.

ents approximately 7.8% of the global carbon pool of 2358 Pg C (i.e., 8.5% of the global vegetation pool of 833 Pg C and 7.4% of the global soil pool of 1525 Pg C) simulated by Foley (1995) using the DEMETER model and the GENESIS climate model (Thompson and Pollard, 1995). For the LGM, the size of the total terrestrial carbon pool estimated for China represents only about 4.8% of the global carbon pool of 1402 Pg C (i.e., 3.3% of the global vegetation pool of 476 Pg C and 5.7% of the global soil pool of 926 Pg C) reconstructed by Van Campo et al. (1993) using LGM CLIMAP palaeodata. Finally, we note that there are several available estimates of the global carbon storage for the present, MH and LGM; we chose to look at only one of them as a baseline, because our objective was to evaluate the relative contribution of China to the global carbon cycle.

4. Discussion

Estimation of terrestrial carbon storage for selected past periods ranging from glacial to interglacial conditions should help to better evaluate the rôle of the terrestrial biosphere in the long-term global carbon cycle, as well as to quantify and separate changes due to natural variability from those due to human activities. Much effort has been exerted to reconstruct global and regional LGM and MH terrestrial carbon budgets (Table 6). On a glacial-interglacial time scale, Shackleton (1977) was the first to suggest that changes in the $\delta^{13}C$ of deep ocean water, seen in benthic forams, might reflect changes in the total amount of carbon stored in biomass and soil. The previously published reconstruction of $\delta^{13}C$ of glacial deep ocean is about 0.32‰ (parts per thousand) (Duplessy et al., 1988). This implies that terrestrial carbon storage during the LGM was 400–500 Pg C less than at present. This estimate was recently updated by Crowley (1995) to 0.40‰, equivalent to about 610 Pg C of glacial-interglacial carbon storage. Simulations using atmospheric general circulation models and various bioclimatic approaches yielded estimates for a global post-LGM increase in carbon storage

Table 6. *Summary of changes in terrestrial carbon storage since the last glacial maximum (LGM)*

Methods	Scale	Results (present − past)	Increase (+) or decrease (−)	References
I. Present — LGM:				
(a) GCM simulations				
GCM + bioclimatic scheme	globe	0 ± 50 Pg(10^{15} g)	+0%	Prentice and Fung (1990)
GCM + bioclimatic scheme	globe	≈300 Pg	+15%	Friedlingstein et al. (1992)
GCM + BIOME model	globe	300–700 Pg	+15%–30%	Prentice et al. (1993)
	globe	≈149	8.8%	Esser and Lautenschlager (1994)
GCM + bioclimatic scheme	globe	612 ± 105 Pg	+23%–33%	Friedlingstein et al. (1995)
(b) Data-based estimates				
marine carbon isotopes change	globe	400–500 Pg	+20%–25%	Duplessy et al. (1988)
	globe	270–720 Pg	+14%–36%	Bird et al. (1994)
mapping LGM vegetation	globe	1350 Pg	+58%	Adams et al. (1990)
	globe	750–1050 Pg	+32%–45%	Crowley (1995)
	globe	715 Pg (430–930) Pg	+33% (20–44%)	Van Campo et al. (1993)
	Africa	154 Pg	N/A	Branchu et al. (1993)
(c) Carbon model and paleodata estimates				
OBM model + paleodata	N. H. (globe)	330–710 Pg (470–1014 Pg)	+21%–44%	Peng et al. (1995a)
	China	90 Pg	+57%	this study
II. Present — MH				
GCM + DEMETER model	globe	−35 Pg	−1.5%	Foley et al. (1995)
Pollen data + biosphere model	Europe	-3.0 ± 0.7 Pg	−1.9%	Peng et al. (1995b)
Paleovegetation data	Siberia	-19.1 ± 3.1 Pg (biomass only)	−22%	Monserud et al. (1995)
OBM + paleodata	China	−27 Pg	−17%	this study

GCM: general circulation model; CLIMAP: climate/long range investigation mapping and prediction; DEMETER: dynamic and energetic models of earth's terrestrial ecosystems and resources; OBM: Osnabrück biosphere model; NH: northern hemisphere.

varying from 0 ± 50 Pg (Prentice and Fung, 1990) to 300–700 Pg (Freidlingstein et al., 1992; Prentice et al., 1993; Freidlingstein et al., 1995). The first data-based estimate suggesting an increase of 1350 Pg since the LGM was given by Adams et al. (1990), who used reconstruction of palaeovegetation to produce a global map of the LGM vegetation. An increase of 715 Pg (430–930 Pg) in terrestrial carbon storage from the LGM to present was calculated by Van Campo et al. (1993) using modern and LGM CLIMAP compilations of both land and sea surface conditions. A third estimate of 750–1050 Pg glacial-interglacial change in terrestrial carbon storage was calculated by Crowley (1995) based on a preliminary version of data compiled by Webb (1995). The last two estimates are similar to the recent result of Peng et al. (1995a) based on the combination of palaeodata and an empirical biosphere model, and consistent with both the modeling results of Prentice et al. (1993) and Freidlingstein et al. (1995) and the ocean-based approach (Duplessy et al., 1988; Bird et al., 1994).

Globally, Foley (1995) has used the DEMETER model to estimate differences in terrestrial carbon storage associated with the modern and mid-Holocene climate simulated by the GENESIS global climate model (Thompson and Pollard, 1995). He found that the total carbon storage in the terrestrial biosphere did not change significantly over the last 6000 years BP. However, the possible vegetation and soil feedbacks were not been considered in the climate simulation of GENESIS, which likely underestimated the increases in summer precipitation by an enhanced African summer monsoon (Kutzbach et al., 1996).

In Europe, Peng et al. (1994, 1995b,c) used reconstructions of palaeoclimates and palaeobiomes from pollen data and an empirical biosphere model to estimate potential terrestrial carbon storage over the last 13000 years BP. The results suggest that changes in climate have significantly altered the distribution of terrestrial biomes. However, these changes did not translate into significant changes in carbon storage in the terrestrial biosphere during the Holocene. The largest decrease of terrestrial carbon storage is found during the late-Glacial period mainly due to the persistence of ice sheets and a small extension of forest. We note, however, that changes in peatland carbon storage are not properly accounted for in the model-based estimations of Foley (1995) and Peng et al. (1995a). Based on the reconstruction of palaeovegetation, Monserud et al. (1995) found that Siberian phytomass storage was 22% greater during the mid-Holocene than potential vegetation in present time. Moreover, Branchu et al. (1993) used the palaeogeographic maps of Africa for the LGM and the mid-Holocene (MH) to conclude that the African continent was a net sink for 154 Pg of C during the last deglaciation but became a source of atmospheric CO_2 after 6000 years BP. These last two studies estimated carbon storage by multiplying the estimated area extent of ecosystem types by the corresponding modern carbon density of vegetation, and did not take into account the effects of different climate conditions on carbon density. Some justification for this is provided by the results of Frienlingstein et al. (1995) who indicated that the carbon densities of most forest vegetation for the LGM are within 10% of their present-day values.

In this study, we found that the terrestrial carbon storage in China increased by about 116 Pg (55 Pg in vegetation and 61 Pg in soil) from the LGM to the MH and decreased about 26 Pg (13 Pg in both vegetation and soil) from the MH to the present. Our results are comparable with the estimates of past terrestrial carbon storage of Africa, reported by Branchu et al. (1993), from the LGM to the present. The similarity of the regions may be associated with effects on paleoclimate and vegetation dynamics by a strengthened monsoon system during the early to mid-Holocene (Kutzbach and Guetter, 1986; Li et al., 1988; An et al., 1991; Javis, 1993; Wang and Sun, 1994; Xiao et al., 1995; Kutzbach et al., 1996). Our results are also in agreement with the assumption that the carbon storage in global terrestrial biomass was relatively low during the LGM at about 18000 years BP, increasing considerably to a maximum between 9500 and 4500 years BP and declining to an intermediate amount by the present time (Grove, 1984). Further, the total terrestrial carbon pool estimated in China comprises about 7.2% of the mean global terrestrial carbon pool for the present time, 7.8% for the MH and 4.8% the LGM. This clearly shows that changes in terrestrial carbon storage for China during the last glacial-interglacial period had a important effect on the global carbon cycle.

It is important to note that the variation of the terrestrial carbon storage in China from the LGM to the present time is closely related to the variations in intensity of Asian monsoons which controlled the change in patterns of climate and vegetation (Li et al., 1988; An et al., 1991; Javis, 1993; Wang and Sun, 1994; Xiao et al., 1995). Loess, sedimentologic, and palynologic data showed that the strengthened northwest winter monsoon and weakened southeast summer monsoon during the LGM resulted in a cold and dry climate, which favored the extensions of deserts, steppes and cold coniferous forests in northern China, and the disappearance of the tropical monsoon rain forests in southern China. The annual average temperature in North China may have been 10–12°C lower than it is now, and annual precipitation may have been about 50% less than its present values (An et al., 1991). In contrast, an enhanced summer monsoon with a warm humid climate resulted in the development of tropical monsoon rain forests and deciduous forest from the LGM to MH. In fact, reconstructions of the mid-Holocene (Shi et al., 1993) show that vegetation moved north and west mainly due to the northward and westward expansion of the summer monsoon, and the annual mean temperature was higher than today by about 1°C in southern China, 2°C in central China, and 3°C in northern and northeast China. The strongest warming of 4–5°C was recorded in the Tibet Plateau (Qinghai-Xizang). Precipitation was tens to hundreds of millimeters greater than at present and was spatially complex. These palaeomonsoon-driven patterns support the results of global climate model experiments that predict an enhanced monsoon system between 12 000 and 6000 years BP followed by a weakened monsoon system from 6000 years BP to present (Kutzbach and Guetter, 1986; COHMAP members, 1988).

There are still some uncertainties, however, due to several possible sources of error in this reconstruction. The first source of error is the difficulty of accurately reconstructing the palaeovegetation and palaeoclimate from sparse palaeodata, especially in the mountain regions. More accurate palaeovegetation maps and palaeoclimate reconstructions for China would improve our estimates, but such maps and climatic reconstructions are not available or published. For now the paleovegetation maps of An et al. (1991) and Shi et al. (1993) remain the standard for the LGM and MH in China (Z. T. Guo, personal communication, 1995). It is believed that the rapid development of Quaternary studies in China will soon make much more complete and accurate palaeoenvironmental data available. The second source of error is the lack of systematic soil information for the LGM and MH. Assuming the same soil fertility factors from LGM to present is probably simplistic; this is discussed by Peng et al. (1995a). A third possible source of error is that the OBM is inherently limited. It seems that an improved estimate of the carbon density is obtained by taking into account the effects of past changes in climate and CO_2 fertilization (Peng et al., 1995b), but it is fundamentally a regression-based, empirical model which does not account for possible feedbacks between productivity and decomposition (McGuire et al., 1993). An improved understanding of the dynamic processes of the global carbon cycle and improved global databases of environmental parameters will facilitate our ability to investigate the global carbon budget at finer spatial and temporal scales.

Despite all the possible sources of error discussed above, we conclude from the reconstruction presented here that the changes in climate and in atmospheric CO_2 concentration resulted in an increase in carbon storage of about 116 Pg from the LGM to the MH in China providing a sink for atmospheric CO_2, but a decrease in carbon storage of about 26 Pg from the MH to the present, providing a source for atmospheric CO_2. Our results clearly show that the monsoon-driven changes in climate and shifts in palaeovegetation during the last glacial-interglacial period had an important effect on the long-term carbon dynamics of China which strongly contributed to the global carbon cycle.

5. Acknowledgements

This paper was presented at the Scientific Symposium held in conjunction with the Fourth Scientific Advisory Council for the IGBP, Beijing, China, 23–27 October 1995. We thank G. Esser who kindly provided the low resolution version of the Osnabrück biosphere model (OBM), R. Leemans for providing the revised version of the IIASA climate Database, and Z. T. Guo (Institute of Geology, Chinese Academy Of Science, Beijing) for his discussion and assistance in conducting this work. We also thank J. Guiot and I. Campbell for comments on an earlier draft, and two anonymous reviewers for their valuable suggestions and comments on this manuscript. The ECC EPOCH Program and the Program Environment of the Centre National de la Recherche Scientifique (France) supported this research. C. H. Peng acknowledges receipt of a Visiting Fellowship from the Natural Sciences and Engineering Council of Canada, funded by the Canadian Forest Service.

REFERENCES

Adams, J. M., Faure, H., Faure-Denard, L., McGlade, J. M. and Woodward, F. I. 1990. Increases in terrestrial carbon storage from the last glacial maximum to the present. *Nature* **348**, 711–714.

An, Z. S, Wu, X, Lu, Y., Zhang D., Sun, X. and Dong, G. 1991. A preliminary study of the paleoenvironment changes of China during the last 20 000 year, In: *Quaternary geology and global change* (ed. D. S. Liu), pp. 1–26. Beijing, China (in Chinese).

Barnola, J. M., Raynaud, D., Korotkevitch, Y. S. and Lorius, C. 1987. Vostok ice core provides 160 000 year record of atmospheric CO_2. *Nature* **329**, 408–414.

Bartlein, P. J. 1988. Late-tertiary and quaternary palaeoenvironments. In: *Vegetation history* (eds. B. Huntley and T. Webb III), pp. 113–152. Kluwer, Dordrecht, The Netherlands.

Beerling, D. J. and Woodward, F. I. 1993. Ecophysiological responses of plants to global environmental change since the last glacial maximum. *New Phytol.* **125**, 641–648.

Bird, M. I., Lloyd, J. and Farqhar, G. D. 1994. Terrestrial carbon storage at the LGM. *Nature* **371**, 566.

Borzenkova, I. I. and Zubakov, V. A. 1984. Climatic optimum of the holocene as a model of the global climate of 21st Century. *Meteorol. Gidrolog.* **8**, 69–77 (in Russian).

Branchu, P., Faure, H., Ambrosi, J. P., Van Zinderen Bakker, E. M. and Faure-Denard, L. 1993. Africa as source and sink for atmospheric carbon dioxide. *Global and Planetary Change* **7**, 41–49.

Butzer, K. W. 1980. Adaptation to global environmental change. *Professional Geographer* **32**, 269–278.

COHMAP Members, 1988. Climatic changes of the last 18 000 years: Observations and model simulations. *Science* **241**, 1043–1052.

Crowley, T. J. 1995. Ice age terrestrial carbon change revised. *Global Biogeochemical Cycles* **9**, 377–389.

Duplessy, J. C., Shackleton, N. J., Fairbanks, R. G., Labeyrie, L., Oppo, D. and Kallel, N. 1988. Deepwater source variations during the last climatic cycle and their impact on the global deep water circulation. *Paleoceanography* **3**, 343–360.

Editors of the Teachers College of Northwest China, 1984. Maps of the natural geography of China. Special Publications Maps Office, Beijing, China (in Chinese).

Esser, G. 1984. The significance of biospheric carbon pools and fluxes for the atmospheric CO_2. A proposed model structure. *Progress in Biometeorology* **3**, 253–294.

Esser, G. 1987. Sensitivity of global carbon pools and fluxes to human and potential climatic impacts. *Tellus* **39B**, 245–260.

Esser, G. 1991. Osnabrück biosphere model: structure, construction, results. In: *Modern ecology: basic and applied aspects*, eds. G. Esser and D. Overdick, pp. 679–709. Elsevier Amsterdam, London, New York, Tokyo.

Esser, G. and Lautenschlager, M. 1994. Estimating the change of carbon in the terrestrial biosphere from 18 000 BP to present using a carbon cycle model. *Environmental Pollution* **83**, 45–53.

FAO-UNESCO 1974. *Soil map of the world*, 1 : 5 000 000, vols. I-X, UNESCO, Paris.

Foley, J. A. 1995. The sensitivity of ecosystems to climatic change: simulating the terrestrial biosphere of the mid-Holocene, *Global Biogeochemical Cycles* **8**, 505–525.

Folland, C. K., Karl, T. R. and Vinnikov, K. Ya. 1990. Observed climate variations and changes. In: *Climate Change: IPCC Scientific Assessment*. Houghton J. T. (eds. G. J. Jenkins and J. J. Epharams), pp. 199–238. Cambridge University Press, New York.

Frenzel, B., Pécsi, M. and Velichko, A. A. 1992. *Atlas of paleoclimates and paleoenvironments of the northern hemisphere*. Late-Peistocene-Holocene. Geographical Research Institute, Hungarian Academy of Sciences, Budapest; Gustav Fischer Verlag, Stuttgar, Jena, New York.

Friedlingstein, C., Delire, C., Muller, J. F. and Gérard, J. C. 1992. The climate induced variation of the continental biosphere: a model simulation of the last glacial maximum. *Geophysical Research Letters* **19**, 897–900.

Friedlingstein, C, Prentice, K. C, Fung, I. Y., John, J. G. and Brasseur, G. P. 1995. Carbon-biosphere-climate interaction in the last glacial maximum climate. *J. Geophys. Res.* **100**, 7203–7221.

Gao, Y., Xu, S., Gao, Q. and Zhang, M. 1962. The monsoon regions and their climate in China. In: *Some problems on east asian monsoon* (ed. Y. S. Gao), pp. 49–63, Science Press, Beijing (in Chinese).

Grove, A. T. 1984. Changing climate, changing biomass, and changing atmospheric CO_2. *Progress in Biometeorology* **3**, 5–10.

IPCC, 1995. Climate Change 1995. In: *The science of climate change* (eds. Houghton, J. T., Meira Filho, L. G., Callander, B. A., Harris, N., Kattenberg, A. and K. Maskell), pp. 460. Cambridge University Press, New York.

Jarvis, D. I. 1993. Pollen evidence of changing Holocene monsoon climate in Sichuan Provence, China. *Quaternary Research* **39**, 325–337.

Kellogg, W. W. 1990. Global influences of mankind on climate. In: *Climate Change: IPCC Scientific Assessment* (eds. Houghton, J. T., Jenkins G. J. and Epharams J. J.), pp. 199–238. Cambridge University Press, New York.

Kutzbach, J. and Guetter, P. J. 1986. The influence of changing orbital parameters and surface boundary conditions on climate simulations for the past 18 000 years. *Journal of Atmospheric Science* **43**, 1726–1759.

Kutzbach, J., G. Bonan, J. Foley and Harrison, S. P. 1996. Vegetation and soil feedbacks on the response of the African monsoon to orbital forcing in the early to middle Holocene. *Nature* **384**, 623–626.

Leemans, R. and Cramer, W. P. 1991. *The IIASA database for mean monthly values of temperature, precipitation, and cloudiness on a global terrestrial grid.* Rep. *IIASA Research RR-91-18*, International Institute for Applied System Analysis, Laxenburg, Austria.

Li, J., Feng, Z. and Tang, L. 1988. Late quaternary monsoon patterns on the Loess Plateau of China. *Earth Surface Processes and Landforms* **13**, 125–135.

Lieth, H. 1975. Modeling the primary production of the world. In: *Primary productivity of the biosphere* (eds. Lieth, H. and Whittaker, R. H.), pp. 237–263, Springer Verlag, New York.

Liu, K. B. 1988. Quaternary history of the temperate forest of China. *Quat. Sci. Rev.* **7**, 1–20.

McGuire, A. D., Joyce, L. A., Kicklighter, D. W., Melillo, J. M., Esser, G. and Vorosmarty, C. J. 1993. Productivity response of climax temperate forests to elevated temperature and carbon dioxide: a North American comparison between two global models. *Climatic Change* **24**, 287–310.

Monserud, R. A., Denissenko, O. V. Kolchugian, T. P. and N. M. Tchebakova, 1995. Change in phytomass and net primary productivity for Siberia from the mid-Holocene to the present. *Global Biogeochemical Cycle* **9**, 213–226.

Moore, T. C., W. H. Hutson, N. Kipp, J. D. Hayes, W. Prell, P. Thompson and Boden, G. 1981. The biological record of the ice-age ocean. *Palaeogeogr., Palaeoclimatol., Palaeoecol.* **35**, 357–370.

Olson, J. S., Watts, J. A. and Allison, L. J. 1985. *Major world ecosystem complexes ranked by carbon in live vegetation. A Database, NPD-017.* Carbon Dioxide Information Center, Oak Ridge National Laboratory, Oak Ridge, Tennessee.

Peltier, W. R. 1994. Ice age paleotopography. *Science* **265**, 195–201.

Peng, C. H., Guiot, J., Van Campo, E. and Cheddadi, R. 1994. The vegetation carbon storage variation in Europe since 6000 BP: reconstruction from pollen. *Journal of Biogeography* **21**, 19–31.

Peng, C. H., Guiot, J. and Van Campo, E. 1995a. Reconstruction of the past terrestrial carbon storage of the northern hemisphere from the Osnabrück biosphere model and palaeodata. *Climate Research* **5**, 107–118.

Peng, C. H., Guiot, J., Van Campo, E. and Cheddadi, R. 1995b. The variation of terrestrial carbon storage at 6000 years BP in Europe: reconstruction from pollen data using two empirical biosphere models. *Journal of Biogeography* **22**, 581–591.

Peng, C. H., Guiot, J., Van Campo, E. and Cheddadi, R. 1995c. Temporal and spatial variations of terrestrial biomes and carbon storage since 13 000 years BP in Europe: reconstruction from pollen data and statistical models. *Water, Air and Soil Pollution* **82**, 375–391.

Prentice, I. C., Cramer, W., Harrison, S. P., Leemans, R., Monserud, R. A. and Solomon, A. M. 1992. A global biome model based on plant physiology and dominance, soil properties and climate. *Journal of Biogeography* **19**, 117–134.

Prentice, I. C., Sykes, M. T., Lautenschlager, M., Harrison, S. P., Denissenko, O. and Bartlein, P. J. 1993. Modelling the increase in terrestrial carbon storage after the last glacial maximum. *Global Ecol. Biogeogr. Lett.* **3**, 67–76.

Prentice, K. C. and Fung, I. Y. 1990. The sensitivity of terrestrial carbon storage to climate change. *Nature* **346**, 48–51.

Sampson, R. N, Apps, M., Brown, S., Cole, C. V., Downing, J., Heath, L. S., Ojima, D. S., Smith, T. M., Solomon, A. M. and J. Wisniewski, 1993. Workshop summary statement: terrestrial biospheric carbon fluxes. Quantification of sinks and sources of CO_2. *Water, Air and Soil pollution* **70**, 3–15.

Schlesinger, W. H., and Melack, J. M. 1981. Transport of organic carbon in the world's rivers. *Tellus* **33B**, 172–187.

Schlesinger, W. H. 1985. The formation of caliche in soil of the Mojave Desert, *California. Geochim. Cosmochim. Acta* **49**, 57–66.

Shackleton, N. J. 1977. Carbon 13 in Uvigerina. Tropical rain forest history and the equatorial Pacific carbonate dissolution cycles, In: *The fate of fossil fuel CO_2 in the Oceans* (eds, R. L. N. Anderson and A. Malahoff), pp. 401–427, Plenum, New York, NY.

Shi, Y., Kong, Z., Wang, S., Tang, L., Wang, F., Yao, T., Zhao, X., Zhang, P. and S. Shi, 1993. Mid-Holocene climate and environment in China. *Global and Planetary Change* **7**, 219–233.

Smith, T. M., Cramer, W. P., Dixon, R. K., Leemans, R., Neilson, R. P. and Solomon, A. M. 1993. The global terrestrial carbon cycle. *Water, Air and Soil Pollution* **70**, 19–37.

Sundquist, E. T. 1993. The global carbon dioxide budget. *Science* **259**, 934–941.

Thompson, S. L. and Pollard, D. 1995. A global climate model (GENESIS) with a land-surface-transfer scheme (LSX). Part I: Present-day climate. *Journal of Climate* **8**, 732–761.

Van Campo, E., Guiot, J. and Peng, C. H. 1993. A data-based re-appraisal of the terrestrial carbon budget at the last glacial maximum. *Global and Planetary Change* **8**, 189–201.

Wang, P. X. and Sun, X. J. 1994. Last glacial maximum in China: comparison between land and sea. *Catena* **23**, 341–353.

Winkler, M. G. and Wang, P. K. 1994. The late-quaternary vegetation and climate of China, In: *Global climate since the last glacial maximum* (eds. Wright, H. E., Kutzbach, J. K., Webb III, T., Ruddiman, W. F., Street-Perrott, F. A. & P. J. Bartlein), pp. 221–265, University of Minnesota Press, Minneapolis.

Webb, R. et al. 1995. Bibliography and inventory of sites with information for constructing digital global maps of vegetation distribution 18 000 years BP. NOAA Paleoclimatol. Publ. Ser. Rep. Nat. Geophys. Data Cent. Boulder, Col., in preparation.

Woodwell, G. M., Mackenzie, F. T., Houghton, R. A., Apps, Michael. J., Gorham, E. and A. Davidson, 1995. Will the warming speed the warming? In: *Biotic feedbacks in the global climatic system: will the warming feed the warming* (eds. Woodwell G. M. and F. T. Mackenzie), pp. 393–411. Oxford University Press, New York and Oxford.

Wu, Z., Liu, F., Zhu, Y., Li, Sh., Li. B., He. Sh., Zheng, X., Chen, Ch., Zhou, Y., Zhou, G., Lin, Y. and Hou, X. 1980. *The vegetation in China.* Science Press, Beijing (in Chinese).

Xiao, J., Porter, S. C., An, Z. S., Kumai, H. and Yoshikawa, S. 1995. Grain size of quartz as an indicator of winter monsoon strength on the Loess Plateau of central China during the last 130 000 years. *Quaternary Research* **43**, 22–29.

Xu, X., S. W. Zhang and Zhao, S. 1987. A preliminary study of the vegetation, climate and environment from Wuhu to Jiangyin region since 30 000 years B. P. *Journal of Nanjing University* **23**, 556–574 (in Chinese, with English abstract).

Ye, D. Zh., Lin, H., Liu, D. S., Chen, S. P, Zhang, X. S., Fu, C. B., Hu, D. X., Chen, P. Q. and Ge, Q. S. 1995. (eds.). *China contribution to global change studies.* China Global Change Report no. 2. Science Press, Beijing, China, pp. 1–226.

Zheng, F. 1986. Late quaternary palynological assemblage in Fuzhou Plain. *Taiwan Strait* **5**, 139–147 (in Chinese, with English abstract).

Zinke, P. J., Stangenberger, A. G., Post, W. M., Emanuel, W. R. and Olson, J. S. 1986. *Worldwide organic soil carbon and nitrogen data.* NDP-018, Carbon Dioxide Information Center, Oak Ridge National Laboratory, Oak Ridge, Tennessee.

Zobler, L. 1986. *A world soil file for global climate modeling.* Rep. NASA TM 87802, GISS, New York, NY, 10025.